UTRECHT UNIVERSITY

Graduate School of Natural Sciences
Applied Data Science

Master's Thesis

Layer-Specific Contributions to Priming of Pop-Out Effects in Macaque Cortex: An LFP Power and Functional Connectivity Analysis

First examiner:
Dr. Chris Klink

Candidate:
Kathrin S. M. Ramsmeier

Further examiners:
Dr. Samson Chota
Dr. Jacob A. Westerberg

July 1, 2024

Abstract

Investigating the effects of priming of pop-out in the visual cortex offers valuable insights into neural processing because it can reveal the dynamics of how the cortex handles sensory information. The primary objective of this research was to explore the processing of information in macaque's visual cortical area V4 during priming of pop-out in a visual search task and examine whether there were differences compared to unprimed settings. V4 can be organised in supragranular, granular and infragranular layers, each being differently involved in information processes within V4 or between other areas of the brain. The analysis utilised local field potential (LFP) signals recorded from this area of two macaque's cortex in 27 sessions, using laminar electrodes across 15 channels covering the entire range of cortical layers. This allowed the sampling of different groups of neurons in each session and a layer-specific analysis in V4. Power, phase synchronisation, and information flow dynamics across layer levels in both primed and unprimed states were investigated. Phase synchronisation between cortical layers was measured by calculating pairwise phase coherence, phase locking values (PLV), phase lag indices (PLI) and pairwise phase consistency (PPC) in the frequency band filtered LFP signals, and information flow dynamics were investigated by applying pairwise Granger causality analysis on the LFP signals of the cortical layers.

The results showed a difference in power between unprimed and primed trials across cortical layers, highlighting altered information processing in primed visual tasks and a possible facilitation effect. No notable differences in phase synchronisation and functional connectivity between unprimed and primed settings were observed, suggesting that the underlying coordination between the cortical layers remains consistent and more local within layers.

Contents

1. Introduction

1.1 Background

Understanding the underlying mechanisms of how the brain processes visual information has been a deeply studied topic (e.g., Maljkovic and Nakayama 1994; Brascamp, Blake, and Kristjánsson 2011; Westerberg, Maier, and Schall 2020; Bichot and Schall 2002) and investigating priming of pop-out provides insights into the neural processes of visual input and the adaption of the brain to the exposure of repetitive visual stimuli. It explains how the brain processes information and efficiently optimises its resources. This further helps to study the underlying mechanisms of neuropsychiatric conditions like schizophrenia and ADHD (e.g., L. V. Moran and Hong 2011).
In a visual search experiment, the observer's task is to identify a unique target item among a group of distracting items. The target that "pops out", i.e., a noticeably different object compared to the surrounding objects, draws attention and repetition of the target "primes" the brain (Westerberg and Schall 2021). Knowledge of the underlying attention-driving feature changes the approach used to complete the search task in subsequent trials. This mechanism is passive and unconscious, improving both accuracy and response time (Maljkovic and Nakayama 1994).
The visual cortex has a hierarchical structure: complex features are processed in higher-level areas, and propagating information from higher to lower areas is achieved through feedback (top-down) processes. Simpler features are processed in lower cortical areas, and feedforward (bottom-up) processes drive neurons in higher regions so that these areas can integrate information and construct more complex receptive field properties (Klink et al. 2017). In V4, the supragranular layers (layers II and III) are mainly involved in feedback processes. They receive input from higher visual areas (Klink et al. 2017) and are responsible for goal-directed mechanisms like

attention (McMains and Kastner 2011), feature integration, and combining various sensory inputs (Westerberg and Schall 2021). The granular layer (layer IV) predominantly receives feedforward inputs from lower visual areas. It mainly processes simpler features and forwards information to the supragranular and infragranular layers (Klink et al. 2017). The infragranular layers (layers V and VI) are part of the feedforward and feedback processes. They forward information to higher visual areas, get feedback for feature integration, and are responsible for combining various sensory inputs (Westerberg and Schall 2021). Feedforward processes are responsible for stimulus-driven mechanisms, such as identifying parts that stand out in the field of vision (McMains and Kastner 2011), and parallel feature processing (Westerberg and Schall 2021). See Figure 1.1 as an illustration.

Priming, in general, can be stimulus-driven as well as object- and goal-related. Thus, priming cannot be classified as solely influenced by bottom-up mechanisms and depends on the specific task (Rauss and Pourtois 2013). Whereas specifically, in priming of pop-out, the attention-focusing target stands out on the basis of a single feature, resulting in fast and automatic processes, and features do not need to be bound and integrated for target identification. Therefore, bottom-up influences are likely the driving mechanisms in priming of pop-out (Westerberg and Schall 2021).

This research aims to identify the cognitive processes associated with priming of pop-out and evaluate the influence of cortical microcircuits organised in layers on processing visual tasks.

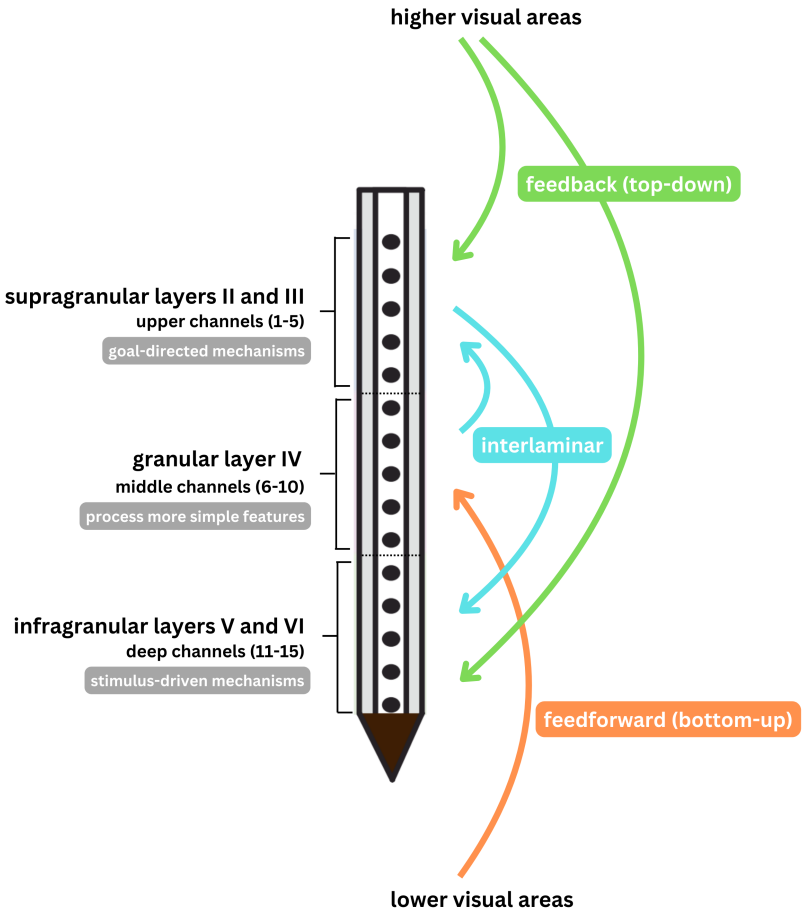

Figure 1.1: Layer illustration of electrodes positioned in V4. Electrode's upper channels (1-5) correspond to supragranular layers II and III, middle channels (6-10) to granular layer IV and deep channels (11-15) to infragranular layers V and VI. The arrows represent feedforward processes (orange) that drive neurons from lower to higher regions, feedback processes (green) that shift neurons from higher to lower regions and intracortical processes (turquoise).

Not all types of repetition yield improvements in accuracy and response time. Attentional selection is faster in situations of priming of pop-out when the target and distractor features are repeated, and it is slower when the target location is repeated, i.e., inhibition of return (Bichot and Schall 2002, Westerberg, Maier, and Schall 2020).

Maljkovic et al. found that target colour had a greater facilitation effect (Maljkovic and Nakayama 1994), whereas other studies did not find a significant difference in the magnitude of the contributions of target enhancement and distractor suppression (Bichot and Schall 2002). Priming can be observed for a period of about half a minute, where the influence weakens

gradually over consecutive trials (Maljkovic and Nakayama 1994).

1.2 Research Focus

This research aimed to examine whether there are differences in how the brain processes information during pop-out searches in unprimed and primed conditions. Compared to previous studies, this study further investigated layer-specific characteristics in V4 to gain detailed insights into the information flow processes. The power and phase characteristics in different frequency bands across the depth of the cortex in area V4 in two macaques were explored in multiple sessions. Each session consisted of recordings from laminar electrodes across 15 channels covering the entire range of cortical layers (again, see Figure 1.1 as an illustration). The characteristics were compared between unprimed and primed settings.

Power analysis was used to evaluate the amplitude of neural oscillations in the different frequency bands, which aimed to give clarity about the underlying neural activity, and by comparing unprimed and primed power spectra, differences in the neural dynamics in V4 were examined. This was further used to investigate layer-specific neural activity. Previous studies (e.g., Maier et al. 2010) found that gamma band activity (>30 Hz) was highest in supragranular layers (in V1). Our analysis aimed to further give insights into how priming of pop-out influences the processing of visual input across different cortical layers in V4.

Phase synchronisation analysis was applied to investigate the coordination of neural oscillations across supragranular (layers II and III), granular (layer IV) and infragranular (layers V and VI) layers, essential for information integration. By calculating different phase synchronisation measures, it was investigated whether the underlying mechanisms were different in priming of pop-out.

Further investigations on how the cortical layers influenced each other were made to observe insights into the underlying cognitive processes and to investigate the layer-specific operations in detail. For this purpose, a Granger causality analysis was conducted to assess how supragranular, granular,

and infragranular layers influenced each other and whether this was different in primed situations. We aimed to see whether the processes were mainly feedforward or feedback and if priming of pop-out changed this behaviour. This indicated how each of the layers in V4 contributes to the information-shifting process in unprimed and primed conditions.
To summarise, we aimed to observe how power, phase synchronisation, and Granger causality in cortical layers were modulated by priming and linked the results to findings in the literature to describe the underlying processes.
The thesis is structured as follows: Chapter 2 provides a description of the data used for the analysis. Chapter 3 describes the methodology used for data processing and analysis. Chapter 4 presents the results. Finally, Chapter 5 reviews the outcomes of the analysis in the context of literature.

2. Data

Local field potential (LFP) signals in V4 in 15 cortical channels were recorded by J. A. Westerberg (Westerberg, Maier, and Schall 2020) from two male Macaca radiata performing a pop-out visual search task with the colour as the relevant feature. This was done in 19 and 8 sessions for the two macaques, each session on a different day. The sessions consisted of multiple trials where the macaques were shown an array of one outstanding target dot of red or green and five distractor dots in the other colour. In each trial, the object representing the target was randomly relocated. The trials were organised in blocks, and the target and distractor colours were held constant within each block and swapped at the end of each block (see Figure 2.1 as an illustration). This study design resulted in the possibility of observing unprimed trials, corresponding to the first two trials within a block, and primed trials, i.e., the remaining ones within the block before the colours were switched. When the macaque moved their gaze to the target, it was rewarded with juice; otherwise, it was not, motivating the macaque to participate (Westerberg, Maier, and Schall 2020).

The LFP signals were measured at 15 cortical channels on a laminar electrode with the electrodes orthogonal to the cortical surface to span the different cortical layers, resulting in 15 time series for each trial (see Figure 2.2 as an example). The electrodes were positioned consecutively in V4 at 0.1mm intervals, ranging from 0mm to 1.4mm. The reference point was channel 10, such that ca. 1mm of cortex above channel 10 and ca. 0.5mm below channel 10 were included (Westerberg, Maier, and Schall 2020). The measurements of channels 1 to 5 resembled the supragranular layers (layers II and III), channels 6 to 10 resembled the granular layer (layer IV), and channels 11 to 15 resembled the infragranular layers (layers V and VI). The sampling rate was 1017.253 Hz (Westerberg, Maier, and Schall 2020).

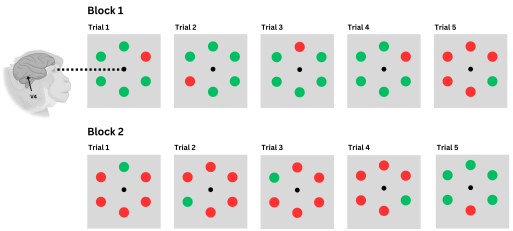

Figure 2.1: Example illustration of the structure of the visual search task. The trials were organised in blocks, and the target and distractor colours were held constant within each block and swapped at the end of each block.

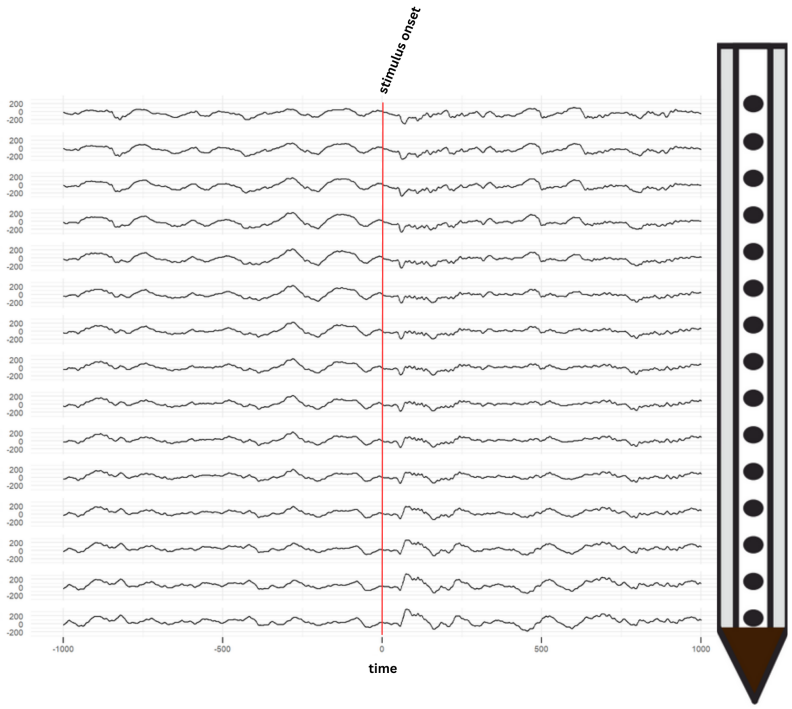

Figure 2.2: LFP signal of a sample trial over time measured at 15 cortical channels using electrodes to span the different cortical layers.

3. Methods

3.1 Data Preprocessing

Baseline corrections were applied to the data by J. A. Westerberg (Westerberg, Maier, and Schall 2020). For this research, the LFP signals between stimulus onset and the macaque's reaction (i.e., the eye movement) were investigated, and only trials where the macaques moved their gaze to the correct item, i.e., the attention-focusing feature, were considered.
During a cognitive task, the macaque brain's activity changes very quickly, leading to non-stationary LFP signals (Kamiński et al. 2001). However, an assumption for Granger causality analysis, which will be utilised, is that the data is (weakly) stationary, meaning that each time series's mean and variance are stable over time (Seth 2010). To achieve this, only the LFP signals after stimulus onset up until 10 milliseconds before the eye movement were considered. Moreover, several steps following Seth 2010; Seth, Barrett, and Barnett 2015; Kamiński et al. 2001 and Ding, Bressler, et al. 2000 were applied to improve stationarity in the LFP signals. In more detail, the following procedure was done for each session:

1. Removal of possible linear trends by detrending each trial.
2. Removal of the temporal mean and division by the temporal standard deviation (z-scoring): The mean of each LFP trial was subtracted from each time point, and each resulting time point was then divided by the standard deviation of the trial, such that the LFP signal in each trial was given equal weight.
3. LFP measures are known to be susceptible to line noise (Seth 2010). Subsequently, line noise was removed using a 60 Hz notch filter. The best filter order was determined for each trial by minimising the ratio of non-stationary trials. The filter order that led to the minimal per-

centage of non-stationary trials identified doing an Augmented Dickey-Fuller test was then used for the final notch filter. In detail, each trial without a notch filter and a range of filter orders from 1 to 20 were tested for stationarity. It is known that by not removing line noise, Granger causality analysis can be disrupted. However, notch filters can also induce casual network artefacts, but these are less severe, and higher MVAR model orders can reduce these artefacts (Seth 2010).

An Augmented Dickey-Fuller test was conducted to measure non-stationarity, where the null hypothesis resembled non-stationarity, and a significance level of 0.05 was used. Furthermore, stationary LFP signals typically have an autocorrelation that sharply declines with increasing lags (Seth 2010). Therefore, the autocorrelation function of various sample trials was examined by investigating the corresponding autocorrelation plots as a helpful tool in detecting non-stationarity.

3.2 Frequency Bands

The following methods were used to analyse power and phase synchrony in the different frequency bands associated with different cognitive states to get insights into the underlying processes between unprimed and primed conditions. The discrete frequency bands were chosen as follows: theta (4–8 Hz), alpha (8–12 Hz), beta (12-30 Hz) and gamma (>30 Hz) (L. V. Moran and Hong 2011). The specific filtering methods are described in the following sections.

3.3 Analysis of Cortical Layer and Priming Status Dependent Induced Spectral Power

Analysing power in the aforementioned frequency bands aimed to get insights into the underlying processes between unprimed and primed conditions. Each trial was first Hanning windowed and then fast Fourier transformed to observe the power spectra. A window (or tapering) function is

a function that returns non-zero values inside and zero values outside an interval (Podder et al. 2014). The Hanning window was chosen because it is known to be a good choice to control for leakage, which could distort frequency domain representations if it was not controlled for (Braun 2001). A window length of 1.5 times the minimum duration that is required to obtain the lowest frequency of interest, i.e., 4 (the lower bound of the theta band), was chosen to observe good frequency resolution while at the same time not distorting the signals. These Hanning windowed signals were then fast Fourier transformed to obtain the frequency content by transforming the signals from their time domain into their frequency domains (Nussbaumer 1982; Heideman, Johnson, and Burrus 1985). To calculate the power within each frequency band, frequency bins, i.e., the frequencies at which the power spectrum was calculated, were defined. These frequency bins ranged from 0 to the Nyquist frequency, i.e., half of the sampling rate. The Nyquist-Shannon sampling theorem states that to reproduce the waveform accurately, the signal has to be sampled twice its highest frequency (Shannon 1949). This means that half the sampling rate, i.e., the Nyquist frequency, is the highest frequency that can be accurately represented. Hence, in the case of the used data with a sampling rate of 1017.253, $1017.253/2 = 508.6263$ was the highest frequency that could be examined.
The spacing between the frequency bins, i.e., the frequency resolution, corresponded to the ratio of the sampling rate to the length of the given LFP trial.
As a next step, the total power corresponding to the sum of power values of the frequency bins was calculated within each frequency band.
This procedure was applied to all LFP signals in all 15 cortical channels in unprimed and primed trials. The mean bands power in each channel was calculated, resulting in each 15 power values for the 4 different frequency bands for both unprimed and primed trials. The calculations were done for all sessions and then averaged.

3.4 Phase Synchronisation Analysis - Phase Coherence, PLV, PLI and PPC

Phase describes the angle corresponding to the momentary deflection of an oscillation or the position within a cycle at a moment in time (Fell and Axmacher 2011). If the rhythms of two LFP signals coincide, the signals are said to be synchronous and prior analyses showed that the emergence of phase synchronisation correlates with attentive and perceptuomotor behaviours (Varela et al. 2001). Phase synchronisation analysis gives insight into how the different cortical layers in V4 coordinate their activity for information processing. By comparing unprimed and primed phase synchronisation outcomes, it can be evaluated how priming affects phase synchronisation patterns and if priming might alter these patterns to improve efficiency.
Multiple metrics can be used to quantify phase synchronisation, including phase coherence, PLV, PLI and PPC.

Phase coherence was calculated to measure the consistency of the phase relationship in the cortical layers. As a first step, each LFP trial was filtered in the different frequency bands using a bandpass Butterworth filter with filter order 2, as this worked best for all trials. A Butterworth filter had the property that the frequency response in the passband was maximally flat, providing a consistent output (Kyu, Aung, and Naing 2009). The filter was applied forwards and backwards (zero-phase filtering) to correct for phase shifts and, therefore, for phase distortion (Ang, Krichane, and Sim 2006). This resulted in the frequency-filtered LFP trials $s_i(t)$.
The auto spectral densities ASD_1 and ASD_2 of pairs of frequency band filtered signals, and the cross-power spectral density CSD between these two frequency band filtered signals were calculated. The phase coherence was then obtained by calculating

$$C = \frac{| \, CSD \, |^2}{ASD_1 * ASD_2} \tag{3.1}$$

Where | CSD | corresponds to the magnitude of the cross-power spectral density (Vinck et al. 2010). The phase coherence C takes values between 0 and 1, where 0 means that no phase synchronisation exists between the two signals at the given frequency, and 1 resembles a perfect phase synchronisation and totally coordinated oscillatory activity (Koopmans 1995).
This was calculated between all channels for all unprimed and primed trials to get $C_{unprimed}$ and C_{primed} in each frequency band.
A limitation is that classical tools for measuring coherence based on Fourier transformations require stationarity (Le Van Quyen et al. 2001). To tackle this problem, various stationarity transformations were applied to the LFP signals, as mentioned in Chapter 2.2. However, some remaining non-stationary LFP signals were still present. Further, phase coherence can't distinguish between the effects of amplitude and phase between two signals since it is a measure of spectral covariance. Therefore, phase coherence can't explicitly be used to say whether phase synchronisation is the relevant mechanism of brain integration and only provides a rough indication (Le Van Quyen et al. 2001). Therefore, further measures, i.e., the phase locking value (PLV), phase lag index (PLI) and pairwise phase consistency (PPC), were calculated to get a deeper insight.

The formulas of Aydore, Pantazis, and Leahy 2013; and Vinck et al. 2010 were applied in R in the following way:
To obtain the analytical signals $z_i(t)$, the frequency-filtered LFP trials $s_i(t)$ were Hilbert transformed by convoluting the signal with the function $\frac{1}{\pi t}$ (Le Van Quyen et al. 2001). The pairwise relative phase or phase difference

$$\Delta\phi(t) = arg(\frac{z_1(t)z_2^*(t)}{\mid z_1(t) \mid\mid z_2(t) \mid}) \tag{3.2}$$

was calculated between all cortical channels and for each frequency band (Aydore, Pantazis, and Leahy 2013). The **phase lag value (PLV)** between

two signals was then obtained from

$$| \mathrm{E}(exp(i\Delta\phi(t))) | \tag{3.3}$$

where $i = \sqrt{-1}$ (Vinck et al. 2010; Aydore, Pantazis, and Leahy 2013).
The PLV ranges from 0 to 1, with 0 indicating no phase synchrony and 1 indicating a consistent relative phase between two signals.
The **phase lag index (PLI)** between two signals was calculated as

$$| \mathrm{E}(sign(\Delta\phi(t))) | \tag{3.4}$$

(Aydore, Pantazis, and Leahy 2013).
The reason for investigating both PLV and PLI was that nonzero PLV values can occur from a single source, influencing both signals. This could happen because the LFP electrode also detects signals from neurons located close to the measured neurons, leading to a single source contributing to both signals. This would result in no phase lag between the two signals and, therefore, in a large PLV value, which would lead to the wrong detection of phase locking between distinct signals, although the aforementioned properties were the decisive underlying mechanisms. Therefore, PLI was additionally used to investigate phase synchronisation, which was zero in the given case. It accomplishes this by focusing on the asymmetry of the phase difference distribution around zero. The PLI will be zero if the analysed LFP signals are linearly mixed from the same source (Aydore, Pantazis, and Leahy 2013), and it will be 1 if perfect phase locking is present (Stam, Nolte, and Daffertshofer 2007). In comparison to phase coherence, Stam et al. found that by investigating different measures of phase synchronisation in multi-channel MEG and EEG, even though phase coherence was just as well suited to detecting changes in synchronisation, PLI was less influenced by common sources (Stam, Nolte, and Daffertshofer 2007).
$\mathrm{PLV}_{\mathrm{unprimed}}$, $\mathrm{PLV}_{\mathrm{primed}}$, $\mathrm{PLI}_{\mathrm{unprimed}}$ and $\mathrm{PLI}_{\mathrm{primed}}$ for each frequency band

were then calculated by averaging over all trials within a session:

$$\text{PLV} = \frac{1}{N} \sum_{n=1}^{N} exp(i\Delta\phi_n(t)) \tag{3.5}$$

$$\text{PLI} = \frac{1}{N} \sum_{n=1}^{N} sign(\Delta\phi_n(t)) \tag{3.6}$$

where N resembles the number of trials (Aydore, Pantazis, and Leahy 2013).

It is further known that phase coherence and PLV give biased estimates for finite sample sizes. Therefore, **pairwise phase consistency (PPC)** was calculated as another alternative measure, which resembles the cosine of the absolute angular distance for all pairs of relative phases. It is, therefore, a measure of how similar the relative phases between two signals are. Since the PPC is based on sequential pairs of observations, it is not biased (Vinck et al. 2010).
For computing the PPC, again, the phase components were extracted from the analytical signals $z_i(t)$ by doing a Hilbert transformation. The pairwise PPC between two cortical channels was then calculated as

$$\text{PPC} = \frac{2}{N^*(N^*-1)} \sum_{j=1}^{N^*-1} \sum_{k=(j+1)}^{N^*} f(\theta_1, \theta_2) \tag{3.7}$$

where

$$f(\theta_1, \theta_2) = \cos(\theta_1)\cos(\theta_2) + \sin(\theta_1)\sin(\theta_2). \tag{3.8}$$

and N^* resembles the length of the phase differences. The PPC ranges between -1 and 1 (Vinck et al. 2010).
$\text{PPC}_{\text{unprimed}}$ and $\text{PPC}_{\text{primed}}$ for each frequency band were then calculated by

averaging over all trials within a session.

3.5 Granger Causality Analysis

To assess whether the influences or communication among the cortical layers were different in unprimed and primed settings, Granger causality analysis was conducted. This analysis is particularly suited for detecting differences in the functional connectivity between experimental conditions, making it a valuable tool for our research. Further, electrophysiological data like LFP signals is well suited to Granger causality analysis because of its high temporal resolution (Seth, Barrett, and Barnett 2015).
The concept of Granger causality is that one can say that a time series X Granger causes a time series Y if the variance of the prediction error of time series Y at the present time is reduced by including past measurements of time series X (Ding, Chen, and Bressler 2006). Granger causality analysis is, therefore, a measure to detect directional influence but does not measure true causality and rather provides a surrogate measure of causal relationships. It reflects a statistical relationship among the observed time series but may not be identical to the underlying physical mechanism (Seth 2010).
To analyse Granger causality, a multivariate autoregressive (MVAR) model for the LFP signals of the 15 cortical channels was created for each unprimed and primed trial. In an MVAR model, the value of a time series at a time point is modelled as a weighted sum of its own past and the past of the other time series. By fitting an MVAR model, the optimal weights are found by minimising the estimation errors (Seth, Barrett, and Barnett 2015). The model order or time-lags of the MVAR model, describing the number of past observations (time-steps) to be included in the MVAR models, is a crucial step in defining the model. The goal is to balance model complexity against error (Seth, Barrett, and Barnett 2015). Too few lags would lead to poor representations of the data and, therefore, underfitting the data, whereas using too many lags would lead to rising model complexity and can further cause overfitting (Seth, Barrett, and Barnett 2015) and problems of model estimation, which might be an issue for trials with a smaller number of data points

(Seth 2010). AIC was used as a first indicator for finding the optimal model order because it is a criterion that balances the variance accounted for by the model against the number of coefficients to be estimated (Seth 2010). It was observed that the AIC monotonically decreased with increasing lags without plateauing, which was also observed in a study by Brovelli et al. (Brovelli et al. 2004). To keep the complexity as small as possible but as large as needed, two different approaches, i.e., using a small model order of 2 for all sessions and using different larger model orders for each session, were applied and compared. To ensure that the MVAR models with the given model orders adequately captured the correlation structure of the LFP signals, several checks were applied following Seth et al. (Seth 2010). The adjusted sum-square error was calculated to assess the amount of variance accounted for by the model, and the MVAR model's consistency was checked (Seth 2010). Further, it was assessed whether there was autocorrelation in the residuals by performing a Portmanteau test and a Breusch-Godfrey test and by investigating residual plots for each cortical channel in randomly sampled MVAR models. The latter also provided a first indication of how to choose the optimal lag order (Battaglia 1990 and Breusch 1978).

The resulting MVAR models were then used to get unconditional Granger causality magnitudes within the MVAR models, which were calculated as the ratio of the variance of the prediction error terms for the MVAR model containing all time series and an MVAR model omitting the potential cause X. If the prediction error for Y of the full MVAR model was significantly smaller than the prediction error of the reduced MVAR model, one could say that X Granger caused Y without accounting for potential influencing signals from other cortical channels (Seth, Barrett, and Barnett 2015).

This analysis was applied pairwise to all 15 cortical channel combinations and evaluated by grouping the results by upper (1-5), middle (6-10) and deep (11-15) cortical channels, resembling supragranular (layers II and III), granular (layer IV) and infragranular (layers V and VI) layers. However, it is important to mention that because unconditional Granger causality was used, it could not be assessed whether the influence between the two

analysed cortical channels was direct or mediated by the other channels (Kamiński et al. 2001).

P-values from an F-Test of the Granger causality magnitudes using a significance level of 0.05 were extracted for each cortical channel pair. To correct for multiple comparisons, the p-values were Bonferroni corrected, which controlled for the expected number of type 1 errors (Seth 2010). A p-value <0.05 meant that the null hypothesis of no causal influence could be rejected. This procedure was then repeated for all unprimed and primed trials within each session to assess whether there were differences between the priming conditions.

A standard Granger causality analysis limitation is that it can only model linear interactions. However, all relevant variance for normally distributed data and most of the relevant variance of approximately normally distributed data can be captured by a linear MVAR model, and nonlinear interactions can sometimes be approximated by a linear MVAR model with a larger model order (Seth, Barrett, and Barnett 2015).

Also, it is crucial to keep in mind that in the presence of unknown (exogenous) or latent variables, the confounding effect on the causal inference cannot be eliminated (Barnett and Seth 2014).

4. Results

The investigation into power as a function of priming status has yielded significant findings. The mean bands power calculated in each cortical channel and for each frequency band was analysed and averaged over all 27 sessions. We observed that power was consistently higher for all frequency bands and cortical layers in unprimed conditions (see Figure 4.1 and Table 4.1). The difference in power between unprimed and primed settings was highest in beta (12-30 Hz) and gamma (>30 Hz) bands. Gamma band activity (>30 Hz) was highest in supragranular layers for both unprimed and primed trials, whereas alpha (8-12 Hz), beta (12-30 Hz) and theta (4-8 Hz) frequencies were higher in infragranular layers than in supragranular layers (see Table 4.1).

To thoroughly investigate the priming effect's influence on the phase relationships between the different layers in the various frequency bands, phase coherence, PLV, PLI, and PPC between the cortical channels within each frequency band were calculated. The results were averaged over all sessions for each measure. Importantly, the differences between unprimed and primed settings for all measures (phase coherence, PLV, PLI and PPC) were very small (<0.1) but consistent over the different sessions. Comparing primed against unprimed conditions, PPC was higher in gamma (>30 Hz) band between all layers and in beta (12-30 Hz) band between all layers but between infragranular and supragranular layers, where the PPC was higher for unprimed compared to primed conditions. Also, in theta (4-8 Hz) bands, PPC was higher in unprimed than in primed conditions for all layers but within infragranular layers. Within infragranular layers, no differences between unprimed and primed conditions were observed. In alpha (8-12 Hz) band, PPC was equal between the priming conditions for all layer levels (see Figure 4.2 C). Results for PLV, PLI and phase coherence were similar.

For both priming conditions, phase coherence for distant cortical layers was lowest in gamma band (>30 Hz) compared to the other frequency bands, and phase coherence was higher in infragranular layers in theta (4-8 Hz), alpha (8-12 Hz) and beta (12-30 Hz) bands than in supragranular layers (see Figure 4.2 A), PLV, PLI and PPC yielded similar results. Further, higher PLI values for theta (4-8 Hz) and alpha (8-12 Hz) than for beta (12-30 Hz) and gamma (>30 Hz) for both unprimed and primed trials were observed (see Table 4.2).

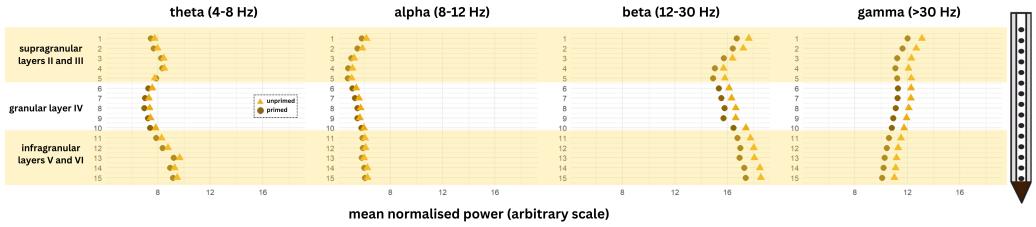

Figure 4.1: Average power in the 15 cortical channels for each frequency band. Lighter triangles resemble unprimed settings, and darker circles resemble primed settings. Upper to deep cortical channels resemble rows 1 to 15 in descending order.

	unprimed setting				primed setting			
	theta (4-8 Hz)	alpha (8-12 Hz)	beta (12-30 Hz)	gamma (>30 Hz)	theta (4-8 Hz)	alpha (8-12 Hz)	beta (12-30 Hz)	gamma (>30 Hz)
supragranular layers	8.1	5.5	16.5	12.5	7.9	5.2	15.8	11.4
granular layer	7.5	5.7	16.6	12.1	7.2	5.4	15.8	11.1
infragranular layers	9.1	6.1	18.2	11.2	8.7	5.9	17.1	10.3

Table 4.1: Mean bands power in unprimed and primed settings grouped for upper (1-5), middle (6-10) and deep (11-15) cortical channels resembling supragranular layers II and III, granular layer IV and infragranular layers V and VI, respectively (rounded to one decimal).

	unprimed setting				primed setting			
	theta (4-8 Hz)	alpha (8-12 Hz)	beta (12-30 Hz)	gamma (>30 Hz)	theta (4-8 Hz)	alpha (8-12 Hz)	beta (12-30 Hz)	gamma (>30 Hz)
min(PLI)	0.75	0.75	0.39	0.17	0.73	0.75	0.39	0.18
mean(PLI)	0.77	0.79	0.48	0.31	0.74	0.79	0.46	0.32

Table 4.2: Minimum and mean PLI in the frequency bands for unprimed and primed settings (rounded to two decimals).

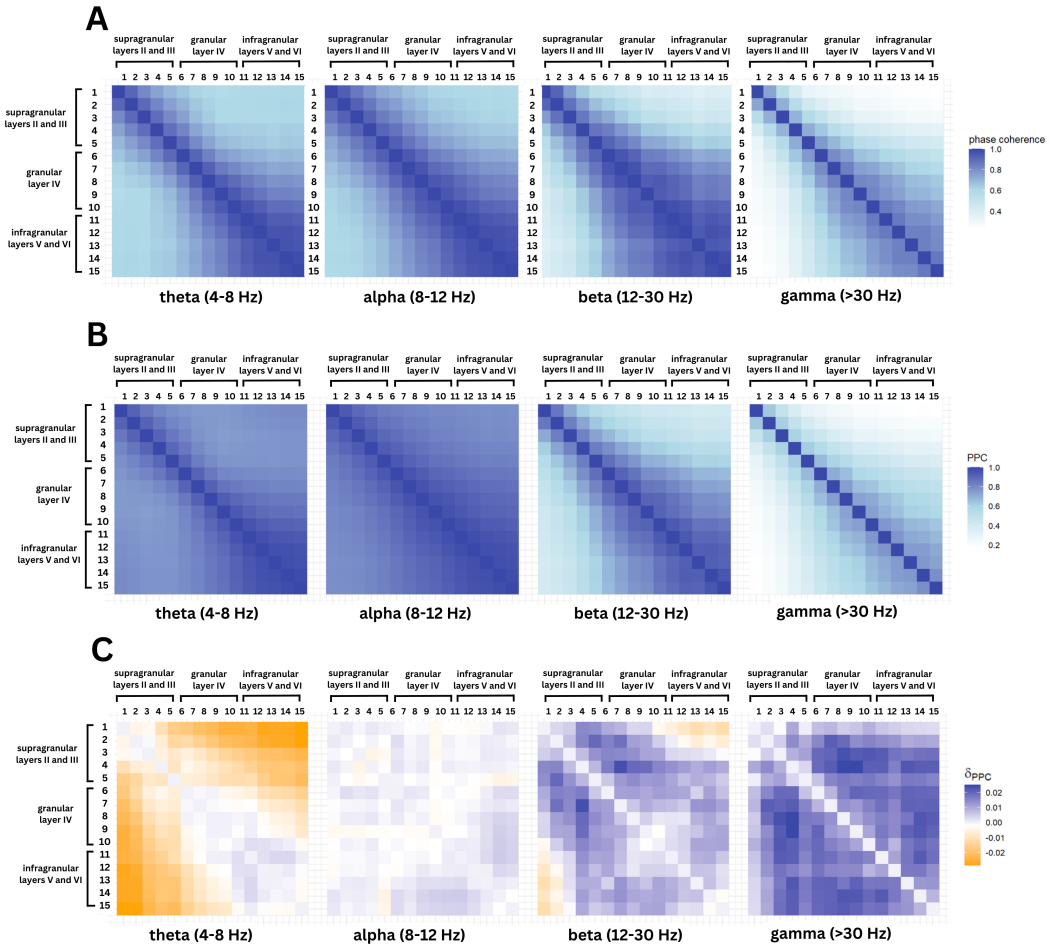

Figure 4.2: Average phase coherence (**A**) and average pairwise phase consistency (PPC) (**B**) in the 15 cortical channels for each frequency band in primed settings. Difference in PPC between unprimed and primed conditions (PPC_{primed} - $PPC_{unprimed}$) (**C**). Upper to deep cortical channels resemble rows and columns 1 to 15 in descending order, corresponding to supragranular layers II and III, granular layer IV and infragranular layers V and VI, respectively. Coherence and PPC are symmetric (by definition), and the results for PLV and PLI were similar.

Further investigating functional connectivity by doing Granger causality analysis (Barnett and Seth 2014) showed no significant differences between unprimed and primed settings (with a maximal absolute difference between unprimed and primed conditions of the ratio of significant Granger causal influences between cortical channels of under 0.1). For both priming states, upper cortical channels (1-5) resembling supragranular layers II and III had the most Granger causal influence on other channels in terms of the percentage of significant Granger causal influences (see Figure 4.3). Deep cortical

channels (10-15) resembling infragranular layers V and VI had the least significant Granger causal influence on supragranular layers, and the most significant Granger causal influences were observed in the direction of supragranular to infragranular layers.

Because non-stationarity is a critical requirement for Granger causality and because some LFP trials remained non-stationary even after applying various transformations mentioned in Chapter 3.1, Granger causality analysis was conducted for both the trials with remaining non-stationarity and after removing them, to check for robustness of the results. No severe differences in the results could be assessed: the ratio of significant Granger causal influences did not change. It was further investigated whether higher MVAR model orders would affect the results, but also no differences were observed.

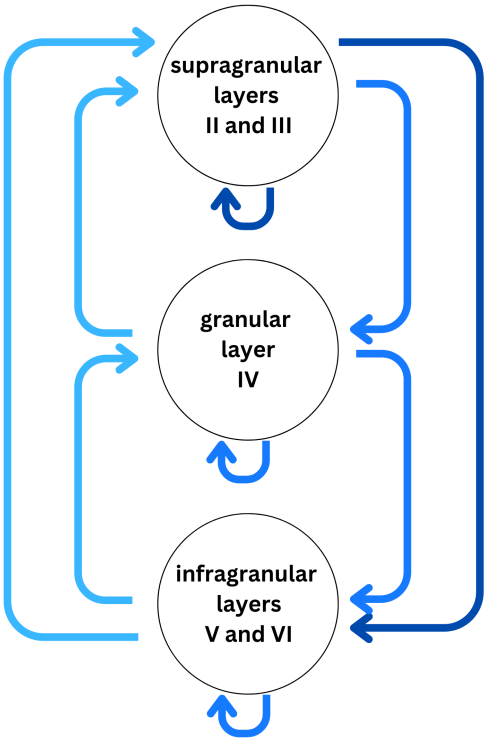

Figure 4.3: Strength of Granger causal directed influences between upper (1-5), middle (6-10) and deep (11-15) cortical channels resembling supragranular layers II and III, granular layer IV and infragranular layers V and VI, respectively, in primed settings. The strength of influence is measured in terms of the ratio of significant Granger causal influences between pairwise cortical channels. Dark blue edges correspond to a stronger influence, and light blue edges resemble a weaker influence. Results in unprimed settings were similar.

5. Discussion

This study sought to determine whether priming of pop-out changed the brain's processing mechanisms investigated in LFP signals recorded during a visual search task in macaques V4. The rationale for this research was based on the assumption that priming modulates neural processing, which can be observed in altered patterns in LFP signals. This helped to perceive the underlying neural mechanisms in priming of pop-out and how repeated exposure to visual stimuli affected the cortical area V4.
Differences were observed in the power spectra, but only small differences were found in phase synchronisation patterns and information flow dynamics in the cortical layers between unprimed and primed settings.

5.1 Power Analysis

In more detail, using power spectral analysis, we observed that power was consistently higher in unprimed conditions for all frequency bands and cortical layers. This indicates that priming of pop-out leads to reduced neural activity (Grill-Spector, Henson, and Martin 2006). The underlying mechanism might be explained by memory trace processes. With each trial, the memory traces weaken, but if there are consecutive trials with the same attention-focusing feature present, i.e., the primed condition, the memory traces do not vanish, and the primed element gets easier to identify, leading to the "pop-out" effect. In unprimed conditions, the memory trace for the attention-focusing feature has not yet been strongly established. More neural activity is needed for target detection, leading to higher LFP power in these unprimed states (Maljkovic and Nakayama 1994).
Gamma band activity (>30 Hz) was highest in supragranular layers (layers II and III) for both unprimed and primed trials, indicating that supragranular layers are important for high-frequency oscillations. Alpha (8-12 Hz),

beta (12-30 Hz) and theta (4-8 Hz) frequencies were mainly observed in infragranular layers (layers V and VI). Consistent with the results, previous studies (e.g., Maier et al. 2010) observed similar outcomes (in V1).
Gamma band activity is associated with perception, attention, memory, consciousness, and motor control (Amo et al. 2017). High gamma activity in supragranular layers suggests that these layers are mainly involved in processing the visual inputs in a visual search task that requires attentional focus, which is in line with the theory discussed in Chapter 1.1 that supragranular layers in V4 are mainly involved in goal-directed mechanisms like attention (McMains and Kastner 2011), feature integration, and combining various sensory inputs (Westerberg and Schall 2021). Theta band activity is mainly involved in memory processes (Herweg, Solomon, and Kahana 2020), alpha band activity is linked to inhibitory processes and attentional suppression and selection, allowing controlled knowledge access (Klimesch 2012) and beta band activity is involved in somatosensory processing and motor control (Barone and Rossiter 2021) and the maintenance of the current sensorimotor or cognitive state (Engel and Fries 2010). Higher activity of theta (4-8 Hz), alpha (8-12 Hz) and beta (12-30 Hz) bands in infragranular layers compared to supragranular layers suggests that infragranular layers are more involved in memory processing, controlled knowledge access and motor planning. Infragranular layers may facilitate the integration of the memory from previous trials with the attention-focusing feature. Controlled knowledge access in infragranular layers may help to get access to information from previous trials, prioritising relevant inputs to improve performance. The motor planning ability, mainly observed in infragranular layers, may contribute to quicker eye movements and further improved efficiency.
However, it is also important to mention that while some studies (e.g., Maier et al. 2010) supported these findings, others detected higher alpha oscillations in supragranular layers, arguing that previous studies were biased due to the lack of using locally specific LFP measurements implicating a more complex distribution of alpha bands (Haegens, Barczak, et al. 2015; Gieselmann and Thiele 2022). This suggests that also the location of recorded

neural activity has a profound influence on the outcome.
Decreased alpha band (8-12 Hz) activity in primed conditions compared to unprimed conditions further suggests promoted processing in task-relevant areas (Haegens, Nácher, et al. 2011), indicating enhanced processing of the visual target stimulus, in terms of standing out more compared to the distractor stimuli.
The biggest differences in band power between unprimed and primed settings in terms of the difference of mean normalised band power grouped for supragranular, granular and infragranular cortical layers occurred in supragranular gamma (>30 Hz) bands (difference of 1.1 grouped mean theta oscillatory normalised power; see Table 4.1) and infragranular beta (12-30 Hz) bands (difference of 1.1 grouped mean beta oscillatory normalised power). These differences in the priming states suggest that priming particularly altered attention, memory, and somatosensory processing.
Supragranular layers are also known to be primarily involved in feedback processes, meaning top-down processes, to receive input from higher brain areas (Klink et al. 2017), and they are responsible for goal-directed mechanisms, like attention (McMains and Kastner 2011). The reduced power, especially in supragranular gamma bands in primed conditions, suggests that these layers may need less neural activity because of better feedback processing and attention modulation.

5.2 Phase Synchronisation Analysis

By analysing the dynamics among the cortical layers, we found that priming did not severely influence the phase synchronisation patterns between the cortical layers. For both priming conditions, phase coherence for distant cortical layers was lowest in gamma band (>30 Hz) compared to the other frequency bands, meaning that the signals measured at distant cortical layers were less synchronised in gamma bands. Supporting these findings, Buffalo et al. did not find spike-field coherence in gamma frequencies in infragranular layers, but they did observe gamma frequencies in the supragranular layers (Buffalo et al. 2011). Our findings suggest that prim-

ing does not strongly influence the synchronisation and coordination of the oscillatory signals. This indicates that, compared to the observed facilitation process measured with calculating power, the underlying coordination between the cortical layers remains consistent and more local.

As discussed in Chapter 1.1, bottom-up influences are likely the driving mechanisms in priming of pop-out (Westerberg and Schall 2021). Bosman et al. and Bastos et al. found that both gamma and theta oscillations are stronger in the bottom-up direction than in the top-down direction (Bosman et al. 2012; Bastos et al. 2015). Alpha oscillatory activity has been associated with top-down directions (Buffalo et al. 2011; Klimesch, Sauseng, and Hanslmayr 2007). Further, Zareian et al. investigated the influence of attention on the LFP phase coherence in rhesus monkeys' visual area MT. They found that with attention, phase coherence increased in low-frequency oscillatory neural activities, indicating improved processing of the stimuli, which was also aligned with faster reaction time to stimulus change. They found the highest attentional modulation of phase coherence in the alpha band (Zareian et al. 2018). Alpha phase synchronisation between task-relevant brain regions is known to increase so neurons can activate common target cells through synchronisation in the alpha band (Klimesch, Sauseng, and Hanslmayr 2007). Buffalo et al. found that the synchronisation of gamma oscillations increased under an attentive state in supragranular layers (Buffalo et al. 2011). This indicates extended processing. They also investigated decreased alpha oscillations under an attentive state in infragranular layers (Buffalo et al. 2011).

We observed higher alpha (8-12 Hz) phase coherence in infragranular layers than in supragranular layers (for both priming conditions). The results are consistent with previous studies by Buffalo et al., which also yielded similar outcomes (Buffalo et al. 2011). This indicates that when the macaque focused on the visual stimuli, this resulted in synchronisation in the alpha band, which corresponded to the top-down process with inhibition of irrelevant stimuli, here especially seen in the infragranular layers.

When subjects withhold or control the execution of a response, event-related synchronisation (ERS) occurs, which can be observed by increasing alpha

band activity. This means that alpha ERS is linked to top-down, inhibitory control processes, such that alpha synchronisation increases when specific actions are suppressed or controlled for, playing an important role in information processing (Klimesch, Sauseng, and Hanslmayr 2007).
However, Bauer et al. observed that alpha modulations increase if the target is more easily predictable and that the enhancement of gamma oscillations decreases (Bauer et al. 2014). This indicates that in primed situations, less attentional adjustment is needed and that alpha oscillations are important for processing predictable input, i.e., input in primed situations, whereas gamma oscillations are more involved in processing new input, i.e., in unprimed situations.
We did not observe significant differences in alpha (8-12 Hz) band phase coherence in unprimed compared to primed settings that would support the findings of either one of the results of the aforementioned studies, indicating no difference in action suppression between unprimed and primed states. We observed a slight increase of gamma (>30 Hz) band phase synchronisation in primed compared to unprimed settings, which does not support the findings of Bauer et al.

5.3 Granger Causality Analysis

To further investigate functional connectivity (Barnett and Seth 2014), Granger causality was chosen for this research since, for other connectivity analyses like dynamic causal modelling (DCM), specific a priori assumptions about the underlying generative mechanisms that produced the data have to be made and are, therefore, less useful for an exploratory analysis (Barnett and Seth 2014) and require specific hypotheses to be tested (Friston, R. Moran, and Seth 2013). Granger causality is also widely used in the field of neuroscience, especially to investigate directional influences among cortical layers in LFP data in the frequency and time domains (e.g., Brovelli et al. 2004; Gieselmann and Thiele 2022; Bosman et al. 2012).
Supragranular layers exhibited stronger Granger causal influence towards infragranular and granular layers rather than in the other directions, and no

significant differences in Granger causal influences were observed between unprimed and primed settings. These findings suggest that deeper layers receive inputs from upper layers in V4, also in primed states and indicate a stable hierarchical structure where higher-order areas guide this processing, and priming seems not to influence these processes. Priming might alter the processing more in individual cortical layers than influence the information flow and communication between layers. The findings that supragranular layers had the most Granger causal influence on other layers align with the theory discussed in Chapter 1.1 and Figure 1.1. Supragranular layers are mainly involved in top-down processes. Therefore, they are important for integrating top-down information, and it might indicate that these layers enhance the processing of relevant features in the other layers in attentive states.

However, the results have to be handled with care. Stokes et al. showed that Granger causality can be highly sensitive to variations in the estimated model parameters. They also found that the Granger causality measure can be biased when using a low model order in the MVAR model. On the other hand, the variance can increase by using a high model order, resulting in spurious peaks in the frequency-domain Granger causalities. To minimise these factors, various tests on the MVAR models and Granger causality analysis on different MVAR model orders were conducted (see Chapters 3.5 and 4). Further, since Granger causality measures both the effects of the source cortical channel and the pathway from that to the influenced cortical channel, the results of Granger causality analysis require a precise understanding of the dynamics of these parts (Stokes and Purdon 2017). This implies that significant Granger causalities can be interpreted as an influence between the signals of two cortical channels, but it does not provide information on how the signals of the cortical channel are influenced. It is further important to mention that in this analysis, unconditional Granger causality was conducted due to the limitations in the used R package. Therefore, it could not be assessed whether the influence between the two analysed cortical channels was direct or mediated by the other channels. (Kamiński et al. 2001).

To summarise, priming of pop-out led to differences in power in all frequency bands and little variation in functional connectivity. Supragranular, granular, and infragranular layers showed different behaviour in the power spectra, and upper cortical layers had the most Granger causal influence on other cortical layers.

References

Amo, Carlos et al. (2017). "Analysis of gamma-band activity from human EEG using empirical mode decomposition". In: *Sensors* 17.5, p. 989.

Ang, Wei Tech, Mounir Krichane, and Terence Sim (2006). "Zero phase filtering for active compensation of periodic physiological motion". In: *The First IEEE/RAS-EMBS International Conference on Biomedical Robotics and Biomechatronics, 2006. BioRob 2006.* IEEE, pp. 182–187.

Aydore, Sergul, Dimitrios Pantazis, and Richard M Leahy (2013). "A note on the phase locking value and its properties". In: *Neuroimage* 74, pp. 231–244.

Barnett, Lionel and Anil K Seth (2014). "The MVGC multivariate Granger causality toolbox: a new approach to Granger-causal inference". In: *Journal of neuroscience methods* 223, pp. 50–68.

Barone, Jacopo and Holly E Rossiter (2021). "Understanding the role of sensorimotor beta oscillations". In: *Frontiers in systems neuroscience* 15, p. 655886.

Bastos, Andre Moraes et al. (2015). "Visual areas exert feedforward and feedback influences through distinct frequency channels". In: *Neuron* 85.2, pp. 390–401.

Battaglia, Francesco (1990). "Approximate power of portmanteau tests for time series". In: *Statistics & probability letters* 9.4, pp. 337–341.

Bauer, Markus et al. (2014). "Attentional modulation of alpha/beta and gamma oscillations reflect functionally distinct processes". In: *Journal of Neuroscience* 34.48, pp. 16117–16125.

Bichot, Narcisse P and Jeffrey D Schall (2002). "Priming in macaque frontal cortex during popout visual search: feature-based facilitation and location-based inhibition of return". In: *Journal of Neuroscience* 22.11, pp. 4675–4685.

Bosman, Conrado A et al. (2012). "Attentional stimulus selection through selective synchronization between monkey visual areas". In: *Neuron* 75.5, pp. 875–888.

Brascamp, Jan W, Randolph Blake, and Árni Kristjánsson (2011). "Deciding where to attend: priming of pop-out drives target selection." In: *Journal of Experimental Psychology: Human Perception and Performance* 37.6, p. 1700.

Braun, S (2001). *WINDOWS. Encyclopedia of Vibration*.

Breusch, Trevor S (1978). "Testing for autocorrelation in dynamic linear models." In: *Australian economic papers* 17.31.

Brovelli, Andrea et al. (2004). "Beta oscillations in a large-scale sensorimotor cortical network: directional influences revealed by Granger causality". In: *Proceedings of the National Academy of Sciences* 101.26, pp. 9849–9854.

Buffalo, Elizabeth A et al. (2011). "Laminar differences in gamma and alpha coherence in the ventral stream". In: *Proceedings of the National Academy of Sciences* 108.27, pp. 11262–11267.

Ding, Mingzhou, Steven L Bressler, et al. (2000). "Short-window spectral analysis of cortical event-related potentials by adaptive multivariate autoregressive modeling: data preprocessing, model validation, and variability assessment". In: *Biological cybernetics* 83, pp. 35–45.

Ding, Mingzhou, Yonghong Chen, and Steven L Bressler (2006). "Granger causality: basic theory and application to neuroscience". In: *Handbook of time series analysis: recent theoretical developments and applications*, pp. 437–460.

Engel, Andreas K and Pascal Fries (2010). "Beta-band oscillations—signalling the status quo?" In: *Current opinion in neurobiology* 20.2, pp. 156–165.

Fell, Juergen and Nikolai Axmacher (2011). "The role of phase synchronization in memory processes". In: *Nature reviews neuroscience* 12.2, pp. 105–118.

Friston, Karl, Rosalyn Moran, and Anil K Seth (2013). "Analysing connectivity with Granger causality and dynamic causal modelling". In: *Current opinion in neurobiology* 23.2, pp. 172–178.

Gieselmann, Marc Alwin and Alexander Thiele (2022). "Stimulus dependence of directed information exchange between cortical layers in macaque V1". In: *Elife* 11, e62949.

Grill-Spector, Kalanit, Richard Henson, and Alex Martin (2006). "Repetition and the brain: neural models of stimulus-specific effects". In: *Trends in cognitive sciences* 10.1, pp. 14–23.

Haegens, Saskia, Annamaria Barczak, et al. (2015). "Laminar profile and physiology of the α rhythm in primary visual, auditory, and somatosensory regions of neocortex". In: *Journal of Neuroscience* 35.42, pp. 14341–14352.

Haegens, Saskia, Verónica Nácher, et al. (2011). "α-Oscillations in the monkey sensorimotor network influence discrimination performance by rhythmical inhibition of neuronal spiking". In: *Proceedings of the National Academy of Sciences* 108.48, pp. 19377–19382.

Heideman, Michael T, Don H Johnson, and C Sidney Burrus (1985). "Gauss and the history of the fast Fourier transform". In: *Archive for history of exact sciences*, pp. 265–277.

Herweg, Nora A, Ethan A Solomon, and Michael J Kahana (2020). "Theta oscillations in human memory". In: *Trends in cognitive sciences* 24.3, pp. 208–227.

Kamiński, Maciej et al. (2001). "Evaluating causal relations in neural systems: Granger causality, directed transfer function and statistical assessment of significance". In: *Biological cybernetics* 85, pp. 145–157.

Klimesch, Wolfgang (2012). "Alpha-band oscillations, attention, and controlled access to stored information". In: *Trends in cognitive sciences* 16.12, pp. 606–617.

Klimesch, Wolfgang, Paul Sauseng, and Simon Hanslmayr (2007). "EEG alpha oscillations: the inhibition–timing hypothesis". In: *Brain research reviews* 53.1, pp. 63–88.

Klink, P Christiaan et al. (2017). "Distinct feedforward and feedback effects of microstimulation in visual cortex reveal neural mechanisms of texture segregation". In: *Neuron* 95.1, pp. 209–220.

Koopmans, Lambert H (1995). *The spectral analysis of time series*. Elsevier.

Kyu, Mya Thandar, Zaw Min Aung, and Zaw Min Naing (2009). "Design and implementation of active filter for data acquisition system". In: *2009 International Conference on Information Management and Engineering*. IEEE, pp. 406–410.

Le Van Quyen, Michel et al. (2001). "Comparison of Hilbert transform and wavelet methods for the analysis of neuronal synchrony". In: *Journal of neuroscience methods* 111.2, pp. 83–98.

Maier, Alexander et al. (2010). "Distinct superficial and deep laminar domains of activity in the visual cortex during rest and stimulation". In: *Frontiers in systems neuroscience* 4, p. 31.

Maljkovic, Vera and Ken Nakayama (1994). "Priming of pop-out: I. Role of features". In: *Memory & cognition* 22.6, pp. 657–672.

McMains, Stephanie and Sabine Kastner (2011). "Interactions of top-down and bottom-up mechanisms in human visual cortex". In: *Journal of Neuroscience* 31.2, pp. 587–597.

Moran, Lauren V and L Elliot Hong (2011). "High vs low frequency neural oscillations in schizophrenia". In: *Schizophrenia bulletin* 37.4, pp. 659–663.

Nussbaumer, Henri J. (1982). "The Fast Fourier Transform". In: *Fast Fourier Transform and Convolution Algorithms*. Berlin, Heidelberg: Springer Berlin Heidelberg, pp. 80–111. ISBN: 978-3-642-81897-4. DOI: 10.1007/978-3-642-81897-4_4. URL: https://doi.org/10.1007/978-3-642-81897-4_4.

Podder, Prajoy et al. (2014). "Comparative performance analysis of hamming, hanning and blackman window". In: *International Journal of Computer Applications* 96.18, pp. 1–7.

Rauss, Karsten and Gilles Pourtois (2013). "What is bottom-up and what is top-down in predictive coding?" In: *Frontiers in psychology* 4, p. 28099.

Seth, Anil K (2010). "A MATLAB toolbox for Granger causal connectivity analysis". In: *Journal of neuroscience methods* 186.2, pp. 262–273.

Seth, Anil K, Adam B Barrett, and Lionel Barnett (2015). "Granger causality analysis in neuroscience and neuroimaging". In: *Journal of Neuroscience* 35.8, pp. 3293–3297.

Shannon, Claude Elwood (1949). "Communication in the presence of noise". In: *Proceedings of the IRE* 37.1, pp. 10–21.

Stam, Cornelis J, Guido Nolte, and Andreas Daffertshofer (2007). "Phase lag index: assessment of functional connectivity from multi channel EEG and MEG with diminished bias from common sources". In: *Human brain mapping* 28.11, pp. 1178–1193.

Stokes, Patrick A and Patrick L Purdon (2017). "A study of problems encountered in Granger causality analysis from a neuroscience perspective". In: *Proceedings of the national academy of sciences* 114.34, E7063–E7072.

Varela, Francisco et al. (2001). "The brainweb: phase synchronization and large-scale integration". In: *Nature reviews neuroscience* 2.4, pp. 229–239.

Vinck, Martin et al. (2010). "The pairwise phase consistency: a bias-free measure of rhythmic neuronal synchronization". In: *Neuroimage* 51.1, pp. 112–122.

Westerberg, Jacob A, Alexander Maier, and Jeffrey D Schall (2020). "Priming of attentional selection in macaque visual cortex: feature-based facilitation and location-based inhibition of return". In: *Eneuro* 7.2.

Westerberg, Jacob A and Jeffrey D Schall (2021). "Neural mechanism of priming in visual search". In: *Attention, Perception, & Psychophysics* 83.2, pp. 587–602.

Zareian, Behzad et al. (2018). "Attention enhances LFP phase coherence in macaque visual cortex, improving sensory processing". In: *BioRxiv*, p. 499756.

A. Appendix

A.1 R Code

The analysis is conducted in R 4.3.2.

`https://github.com/kathrinramsmeier/thesis`

A.2 R Packages

- Bao H (2023). _bruceR: Broadly Useful Convenient and Efficient R Functions_. R package version 2023.9, <https://CRAN.R-project.org/package=bruceR>.
- Borchers H (2023). _pracma: Practical Numerical Math Functions_. R package version 2.4.4, <https://CRAN.R-project.org/package=pracma>.
- H. Wickham. ggplot2: Elegant Graphics for Data Analysis. Springer-Verlag New York, 2016.
- K J Rahim, W S Burr and D J Thomson, Appendix A: Multitaper R Package in "Applications of Multitaper Spectral Analysis to Nonstationary Data," PhD diss., Queen's University, 2014, pp. 149-183, http://hdl.handle.net/1974/12584
- Pfaff, B. (2008) Analysis of Integrated and Cointegrated Time Series with R. Second Edition. Springer, New York. ISBN 0-387-27960-1
- Signal developers (2023). _signal: Signal processing_. <https://r-forge.r-project.org/projects/signal/>.
- Trapletti A, Hornik K (2023). _tseries: Time Series Analysis and Computational Finance_. R package version 0.10-55, <https://CRAN.R-project.org/package=tseries>.
- Van Boxtel, G.J.M., et al. (2021). gsignal: Signal processing. URL: https://github.com/gjmvanboxtel/gsignal
- Wickham H, Averick M, Bryan J, Chang W, McGowan LD, François R, Grolemund G, Hayes A, Henry L, Hester J, Kuhn M, Pedersen TL, Miller E, Bache SM, Müller K, Ooms J, Robinson D, Seidel DP, Spinu V, Takahashi K, Vaughan D, Wilke C, Woo K, Yutani H (2019). "Welcome to the tidyverse." _Journal of Open Source Software_, *4*(43), 1686. doi:10.21105/joss.01686 <https://doi.org/10.21105/joss.01686>.
- Zeileis A, Hothorn T (2002). Diagnostic Checking in Regression Rela-

tionships. R News 2(3), 7-10. URL
https://CRAN.R-project.org/doc/Rnews/